European Spine Journal (2019) 28:1977–1986
https://doi.org/10.1007/s00586-019-06001-5

ORIGINAL ARTICLE

Asymmetric expression of GPR126 in the convex/concave side of the spine is associated with spinal skeletal malformation in adolescent idiopathic scoliosis population

Enjie Xu[1] · Tao Lin[1] · Heng Jiang[1] · Zhe Ji[1] · Wei Shao[1] · Yichen Meng[1] · Rui Gao[1] · Xuhui Zhou[1]

Received: 27 December 2018 / Revised: 24 April 2019 / Accepted: 5 May 2019 / Published online: 11 May 2019
© Springer-Verlag GmbH Germany, part of Springer Nature 2019

Abstract

Purpose To determine the relationship between the bone formation-related functions of GPR126 and the structural asymmetry of spine in adolescent idiopathic scoliosis (AIS).

Methods Vertebral body samples were obtained from 51 AIS patients during spinal surgery between October 2014 and November 2017, and the expression pattern of GPR126 in the convex/concave sides of AIS spine was identified by RT-qPCR. Next, we explored the bone formation-related functions of GPR126 by knocking down and overexpressing GPR126 in human mesenchymal stem cells (hMSC) and further performing osteogenic differentiation. We also applied overexpression of N-terminal fragments derived from GPR126 (GPR126-NTFs) and osteogenic differentiation experiments to determine the functional part of GPR126 in skeletal development.

Results We provided evidence that GPR126 showed a marked convex/concave asymmetric expression in the spine of AIS. Further RNA detection found that exon6-included transcripts of GPR126 (GPR126-exon6^{in}) were significantly higher expressed in the convex side of AIS patients. Knocking down of GPR126 accelerated ossification of hMSCs during osteogenic differentiation, and overexpression of GPR126-exon6^{in} delayed this process. Overexpression of GPR126-NTFs revealed that NTF is a functional fragment and exon6-included NTF (NTF-exon6^{in}) delayed ossification of hMSCs.

Conclusion Our findings indicated that GPR126-NTFs play a role in skeletal development, and the inclusion/exclusion of exon6 may regulate the bone formation-related functions of GPR126. The convex/concave asymmetric expression of GPR126-exon6^{in} may be an important factor in abnormal bone formation of AIS.

Graphical abstract

These slides can be retrieved under Electronic Supplementary Material.

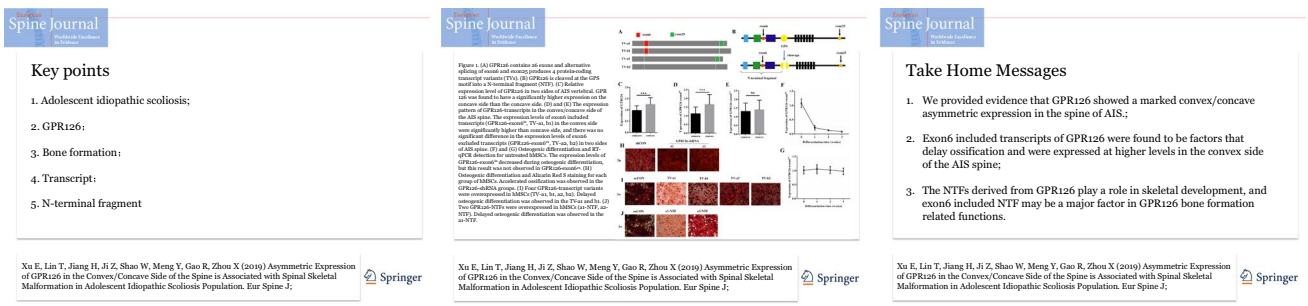

Enjie Xu, Tao Lin contributed equally to this work.

Electronic supplementary material The online version of this article (https://doi.org/10.1007/s00586-019-06001-5) contains supplementary material, which is available to authorized users.

Extended author information available on the last page of the article

Keywords Adolescent idiopathic scoliosis · GPR126 · Bone formation · Transcript · N-terminal fragment

Introduction

Adolescent idiopathic scoliosis (AIS) is a structural tridimensional spinal deformity disease with at least one curve with a Cobb angle greater than 10°. Some researchers have found structural asymmetry between the convex and concave sides of the vertebral body, especially at the apex of the curve [1–3], and the mean bone density of cortical shell and cancellous in the concave side was higher than convex side at the apical vertebra [4]. Abnormal skeletal maturation has been observed in AIS patients [5, 6]. Low bone mass and abnormal bone microstructure were found in patients with AIS and were considered to be important prognostic factors for curve progression of AIS [7–12]. In addition, AIS was associated with less mineralization in bone tissues, lower cortical bone area and volumetric bone mineral density (vBMD), less trabecular number and connectivity, higher trabecular separation and trabecular area [11–13].

GPR126, also named ADGRG6, DREG or VIGR, is a member of adhesion G protein-coupled receptor GPCR family. Genome-wide association study (GWAS) in 1819 Japanese AIS cases and 25,939 controls demonstrated that GPR126 is a susceptibility gene of AIS [14]. Other studies further confirmed the relationship between GPR126 and AIS [15–17]. GPR126 may be associated with bone development. GWAS studies suggest that human height is associated with GPR126 in both children and adults [18–21]. GPR126 was found to be associated with the vertebral ossification in zebra fish [14], and GPR126-null mice have limb posture abnormalities and growth failure [22]. Recently, higher expression of GPR126 in vertebral bone has been reported in patients with AIS [16].

However, there was recently no research to demonstrate the relationship between GPR126 and structural asymmetry of the AIS spine. We speculated that the GPR126 expression levels in the convex/concave sides of the spine may be different and play a role in asymmetric spine formation in AIS patients. We plan to investigate the expression pattern of GPR126 in the convex/concave sides of AIS spine and explore the bone formation-related functions of GPR126 by knocking down and overexpressing GPR126 in human mesenchymal stem cells (hMSC) and further performing osteogenic differentiation.

GPR126 contains 26 exons, and alternative splicing of exon6 and exon25 produces four protein-coding transcript variants. Each transcript variant may have specific functions in skeletal development. GPR126 is cleaved at the G protein-coupled receptor proteolysis site (GPS) motif into a N-terminal fragment (NTF) [23], and NTF works by interacting with neighboring cells or extracellular matrix [24]. The alternative splicing of exon6 produces two NTF variants: exon6-included NTF (NTF-exon6^{in}) and exon6-excluded NTF (NTF-exon6^{ex}). We speculated that one of the NTF variants may be a functional fragment of GPR126 and play a role in bone formation. Asymmetric expression of NTF-exon6^{in} or NTF-exon6^{ex} may be associated with spinal skeletal malformation in AIS.

Materials and methods

Study population and sample collection

A total of 51 adolescent idiopathic scoliosis patients in Shanghai Changzheng Hospital were enrolled in this study between October 2014 and November 2017. The standing posteroanterior radiographs were taken for each AIS patient. Cobb angle of the curves was measured, and the most severe curve was selected if more than one curve was discovered in one patient (Table 1). Vertebral body samples were collected during surgery after obtaining informed consent from all participants or their parents. The study has been approved by the Ethical Committee of Shanghai Changzheng Hospital and conformed to the tenets of the Declaration of Helsinki.

Vertebral body samples were obtained from 51 AIS patients during spinal surgery. All samples were collected at the convex and concave sides of the apex for AIS patients and immediately placed in sterile tubes and stored in liquid nitrogen to avoid RNA degradation.

Cell culture and osteogenic differentiation

Human mesenchymal stem cells (hMSCs) were collected after obtaining informed consent from all donors. We collected hMSCs from seven donors in this study, and these donors did not have any skeletal malformations. A well-grown MSC cell line was selected for knocking down, overexpression, osteogenic differentiation and detection, and experiments were repeated in two other cell lines. DMEM/

Table 1 Characteristics of the study population

Parameter	AIS cases
Ethnic group	Chinese Han
Female/male	44/7
Mean age ± SD (years)	13.7 ± 1.6
Age range (years)	11–17
Mean Cobb angle ± SD (°)	58.2 ± 10.6
Cobb angle range (°)	44–86

F12 (Hyclone, Utah, USA) medium contains 10% FBS (FBS, Gibco, NY, USA), penicillin (100 U/L, Invitrogen, NY, USA) and streptomycin (100 mg/L, Invitrogen, NY, USA). Cells were cultured in DMEM/F12 and placed in a humidified atmosphere of 5% CO_2 at 37 °C.

Osteogenic differentiation of hMSCs was applied by OriCell Human Mesenchymal Stem Cell Osteogenic Differentiation Medium (Cyagen Biosciences, CA, China). Cells were seeded at 2.0×10^3 cells/cm^2 in 6-well culture plates and cultured in complete DMEM/F12 until they reached 60–70% confluence. Next, hMSCs were cultured in osteogenic differentiation medium (osteogenic basal medium containing 10% FBS, 100 nM dexamethasone, 50 μM ascorbate and 10 mM β-glycerophosphate, Cyagen Biosciences, CA, USA). The medium was replaced every 3 days for 3 weeks. After differentiation, the cells were fixed with 4% formaldehyde (Sigma–Aldrich, St. Louis, MO, USA) for 30 min and stained with 1% Alizarin Red S (Sigma–Aldrich, St. Louis, MO, USA) for 5 min at room temperature. The stained cells were rinsed with PBS three times to remove excess stains and photographed.

Knocking down of GPR126

Recombinant lentiviruses knocking down GPR126 expression and blank lentivirus (without knockdown sequence) were purchased from Shanghai GeneChem Co., Ltd. (Shanghai, China), and hMSCs were transfected with knocking down lentiviruses (shRNA) and blank lentivirus (shCON). We determined that the optimal multiplicity of infection (MOI) for MSC virus infection was 30 by pre-experiment and conducted the formal experiments based on this MOI value. In order to increase the proportion of infected cells, we performed flow sorting after 3 days of cell infection and continued to culture the cells with green fluorescence. We extracted RNA and proteins when the cells reached 70–80% confluence. Knocking down efficiency was confirmed by RT-qPCR and Western blot.

Overexpression of GPR126 and NTFs

GPR126 contains 26 exons, and alternative splicing of exon6 and exon25 produces four protein-coding transcript variants. Transcript variant a1 (TV-a1) contains both exon6 and exon25, TV-b1 only contains exon6, TV-a2 only contains exon25, and TV-b2 does not contain any one (Fig. 2a). Recombinant lentiviruses overexpressing four GPR126-transcripts and blank lentivirus (without overxepression sequence) were purchased from Shanghai GeneChem Co., Ltd. (Shanghai, China), and hMSCs were transfected with overexpression lentiviruses (TV-a1, b1, a2, b2) and blank lentivirus (oeCON).

GPR126 is cleaved at the G protein-coupled receptor proteolysis site (GPS) motif into a N-terminal fragment (NTF) [23]. Recombinant lentiviruses overexpressing two GPR126-NTFs and blank lentivirus (without overxepression sequence) were purchased from Shanghai GeneChem Co., Ltd. (Shanghai, China), and hMSCs were transfected with overexpression lentiviruses (a1-NTF, a2-NTF, a1-NTF contains exon6 but a2-NTF does not) and blank lentivirus (oeCON).

After 72-h incubation, the supernatant containing lentivirus was removed and replaced with complete medium. Overexpression efficiency was confirmed by RT-qPCR. It is impossible to detect the expression of each isoform of GPR126 because there are currently no reliable antibodies to distinguish these isoforms.

RT-qPCR

To quantitatively determine the expression level of GPR126, or infection efficiency of each knocking down or overexpression group, GPR126 mRNA, each transcript or NTF sequence was determined by RT-qPCR using SYBR-Premix Ex Taq (Takara, Japan) and ABI Prism 7900HT sequence detection system (Applied Biosystems, Carlsbad, CA). Total RNA of each group was extracted with TRIzol according to the manufacturer's instructions. The mRNA was transcribed into cDNA using a Reverse Transcription kit (Applied Biosystems, Carlsbad, CA). The genes were amplified using specific primers, and human β-actin gene was used as an endogenous control. The PCR primer sequences used were: GPR126: forward: 5′-TGTCGTTAATATCAGTTTTCACC-3′, reverse: 5′-TATGTAGCCTCAAGCCTTCA-3′; exon6-included GPR126-transcripts (GPR126-exon6^{in}): forward: 5′-TACACCACCCACTGTCACCA-3′, reverse: 5′-ATTCTG CCACCTTGCTCTGT-3′; and exon6-excluded GPR126-transcript (GPR126-exon6^{ex}): forward: 5′-GACCCTCTG TCAAGATGGAATTAT-3′, reverse: 5′-CTTGTCCTCTCC AGCACTCAG-3′. Exon6-included GPR126-NTF (NTF-exon6^{in}): forward: 5′-ACTGTCACCACTAACATGCCT-3′, reverse: 5′-TACCTCAGGGTGACGAAGGAT-3′; β-actin: forward: 5′-ACCGAGCGCGGCTACAG-3′, reverse: 5′-CTT AATGTCACGCACGATTTCC-3′ data were analyzed using the comparative Ct method ($2^{-\Delta\Delta Ct}$). In the detection of GPR126 expression in the spine of AIS patients, we repeated the RT-qPCR experiment three times with the same samples and the same primers. In the detection of GPR126 expression in untreated/treated MSCs, we repeated the RT-qPCR experiment three times with the same samples and the same primers, and further repeated all experiments, including knocking down, overexpression, osteogenic differentiation and RT-qPCR detection in two other MSC cell lines derived from different donors.

Western blot assay

GPR126 is a membrane protein. The cells of knocking down group were collected and extracted membrane protein using a Mem-PER Plus Membrane Protein Extraction kit (Pierce, IL, USA). Osteogenic differentiated cells extracted whole protein using a protein extract kit (Beyotime, Shanghai, China), and the concentration was determined by using a BCA Protein Assay kit (Pierce). Equal amounts of cell extracts were run on SDS-PAGE gels. Separated protein bands were transferred onto polyvinylidene fluoride (PVDF, Millipore, MA, USA) membranes and blocked in 5% bovine serum albumin (BSA, Sigma–Aldrich, St. Louis, MO, USA), and membranes were probed overnight at 4 °C with the appropriate primary antibody. Antibody used was as follows: GPR126 (1:500 dilution, ab75356, Abcam, Cambridge, UK), Na^+/K^+-ATPase (1:500 dilution, ab58475, Abcam), alkaline phosphatase (ALP, 1:10,000 dilution, ab133602, Abcam), osteocalcin (BGLAP, 1:500 dilution, ab93876, Abcam) and GAPDH (1:10,000 dilution, ab181602, Abcam). Membranes were then probed with a horseradishperoxidase-conjugated secondary antibody for 1 h at room temperature. The immunoreactive bands were visualized using an enhanced chemiluminescence (ECL) Western blotting substrate (No. 32106, Pierce). We chose loading control according to Abcam recommendation (http://www.abcam.com/primary-antibodies/loading-control-guide). The relative protein level in different cell lines was normalized to Na^+/K^+-ATPase or GAPDH concentration. Three separate experiments were performed for each group.

Statistical analysis

Analysis of the data was performed using SPSS version 23.0, with P value < 0.05 considered statistically significant. All data were presented as the mean ± SD. The Mann–Whitney U test was used to compare the difference of GPR126 expression between the concave side and the convex side of the AIS patients (Figs. 1a, 2b and c). The Kruskal–Wallis H test was used to analyze the differences between groups (Figs. 1b, 2f and 3b).

Results

Characteristics of the patients

Patients enrolled in this study were diagnosed as AIS and had at least one curve of Cobb angle greater than 20°. There were 44 females and seven males in our study, and the mean Cobb angle was 58.2 ± 10.6° (range, 44–86) and mean age was 13.7 ± 1.6 years (range, 11–17). All these patients were Chinese Han (Table 1). Bone tissue samples from the apex region of spine were obtained during spinal orthopedic surgery.

GPR126 plays a role in skeletal development

The qPCR results showed that the expression level of GPR126 in the convex side was significantly higher than concave side (Fig. 1a). We cultured and knocked down the GPR126 expression in hMSCs. The results of qPCR and Western blot indicated that the expression level of GPR126 in GPR126-sh#1 and GPR126-sh#2 was significantly lower than control (Fig. 1b, c). Further osteogenic differentiation experiments were applied to explore the effects of GPR126 in bone formation. The results of Alizarin Red S staining and Western blot showed an accelerated osteogenic differentiation in GPR126-sh#1 and #2 (Fig. 1d, e).

Two transcripts of GPR126 may be associated with bone formation and spinal deformity

Next, we detected the expression pattern of GPR126-transcripts in the convex/concave side of the AIS spine. The expression levels of exon6-included transcripts (GPR126-exon6^{in}, TV-a1, b1) in the convex side were significantly higher than concave side, and there was no significant difference in the expression of exon6-excluded transcripts (GPR126-exon6^{ex}, TV-a2, b2) in two sides of AIS spine (Fig. 2b, c).

To further confirm the associated between GPR126 and skeletal development, we applied osteogenic differentiation and RT-qPCR detection for untreated hMSCs. The expression levels of GPR126-exon6^{in} decreased during osteogenic differentiation, but this result was not observed in GPR126-exon6^{ex} (Fig. 2d, e). Next, we overexpressed four GPR126-transcripts in hMSCs, and osteogenic differentiation experiments were applied later. The results showed that the expression levels of GPR126-exon6^{in} in TV-a1 and b1 were significantly higher than TV-a2 and b2, and delayed osteogenic differentiation was observed in the TV-a1 and b1 (Fig. 2f, g).

Exon6 sequence regulates the bone formation-related functions of NTFs

GPR126 is cleaved at the GPS motif into a N-terminal fragment (NTF) that locates to the plasma membrane [23] (Fig. 3a). Two GPR126-NTFs were overexpressed in hMSCs (a1-NTF, a2-NTF). The results of RT-qPCR and Alizarin Red S staining showed that the expression level of exon6-included NTF (NTF-exon6^{in}) in a1-NTF was significantly higher than a2-NTF, and delayed osteogenic differentiation was observed in the a1-NTF (Fig. 3b, c).

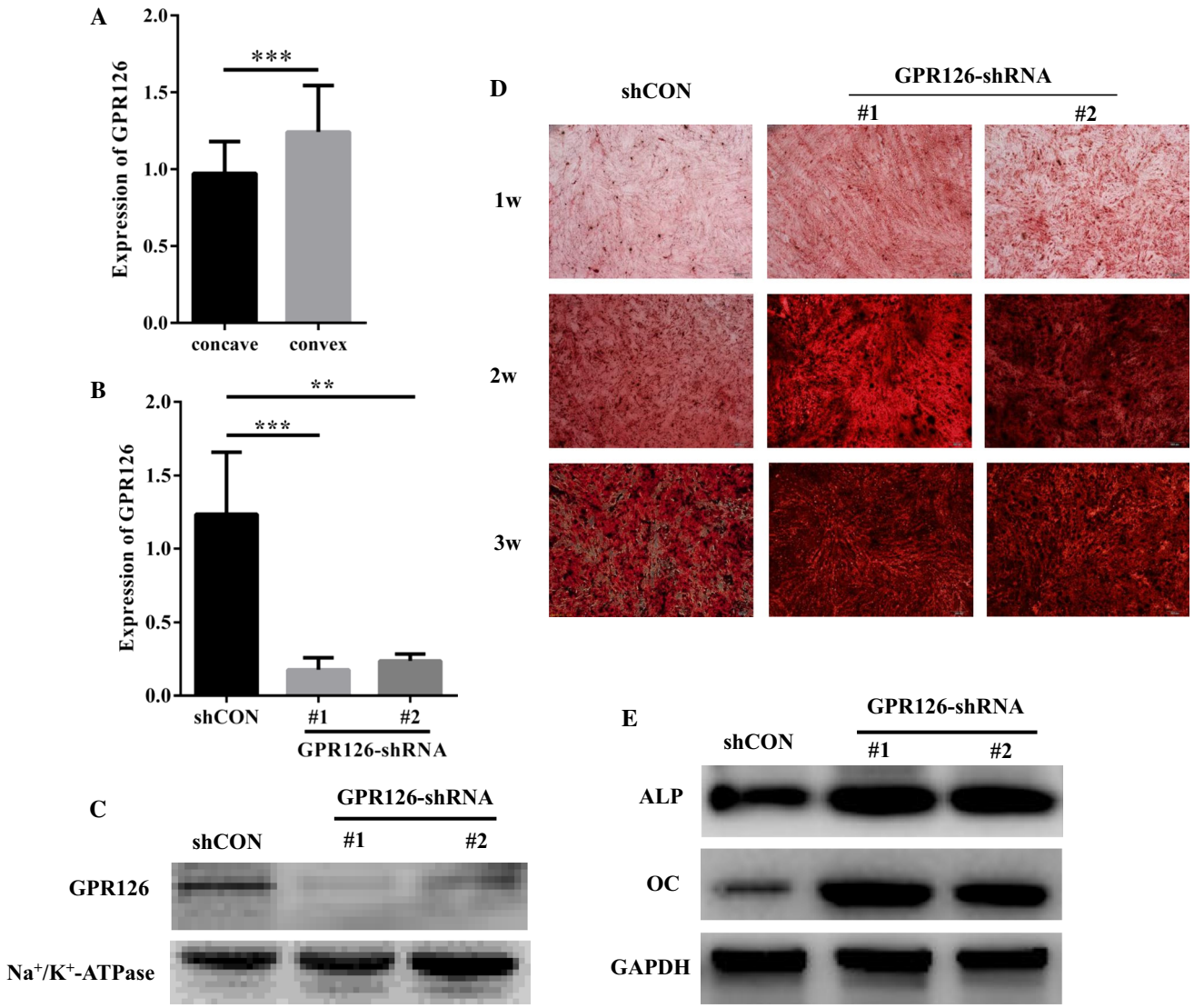

Fig. 1 The bone formation-related factor GPR126 showed a marked convex/concave asymmetric expression in the spine of adolescent idiopathic scoliosis (AIS) patients. **a** Relative expression level of GPR126 in two sides of AIS vertebral body. GPR 126 was found to have a significantly higher expression on the concave side than the concave side. $n=51$. **b** and **c** GPR126 was significantly knocked down in GPR126-shRNA#1 and GPR126-shRNA#2. **d** Osteogenic differentiation and Alizarin Red S staining for each group of hMSCs. Accelerated ossification was observed in the GPR126-shRNA groups. **e** Detection of alkaline phosphatase (ALP) and osteocalcin (BGLAP) expression levels after 3 weeks of osteogenic differentiation using Western blot assay. Higher protein expression levels of ALP and BGLAP were observed in the GPR126-shRNA. Data were presented as the mean ± SD. $^{**}P<0.01$, $^{***}P<0.001$

Discussion

It is evident that there is a strong correlation between AIS and abnormal bone formation. A longitudinal cohort study of 513 girls with AIS supported the relationship between abnormal bone density and the etiopathogenesis of AIS [25]. Low bone mass has been reported in idiopathic scoliosis patients [7–9] and was found to be an important prognostic factor for curve progression in AIS [10]. Tanabe et al. [26] found that minodronate treatment improves low bone mass and reduces progressive thoracic scoliosis in a mouse model of AIS. AIS was found to be associated with lower cortical bone area, cortical bone volumetric BMD (vBMD), trabecular number and higher trabecular separation and trabecular area [11, 13]. Wang and co-workers [12] reported reduced trabecular number and connectivity and less mineralization in bone tissues of AIS patients, which may be due to the down-regulation of Runx2 and up-regulation of Spp1 and TRAP. A CT scan study on 53 female idiopathic scoliosis patients showed a marked convex/concave asymmetry in bone density of spine. At the apical vertebra, the mean bone density of cortical shell

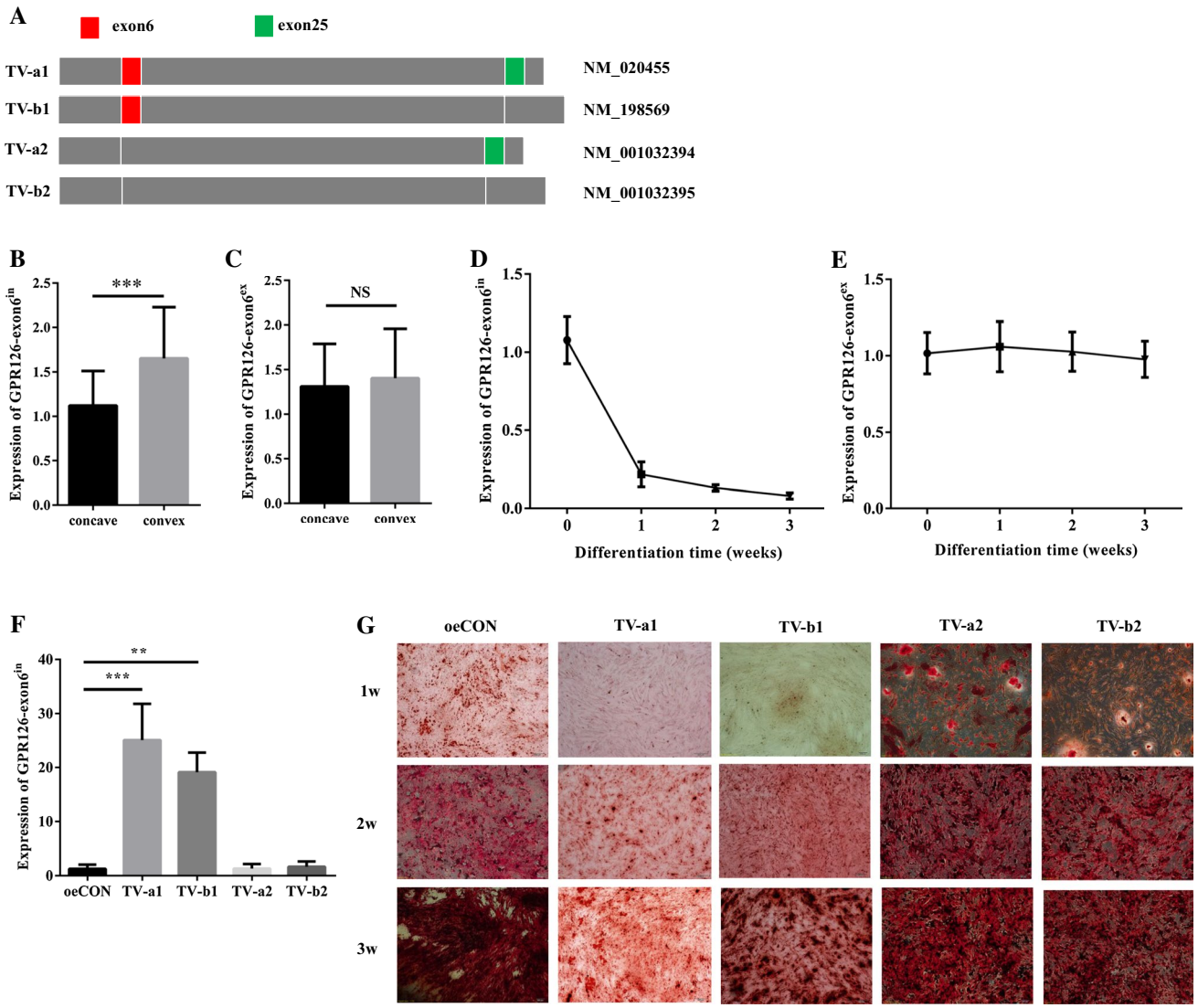

Fig. 2 The expression pattern of GPR126-transcripts in the convex/concave side of the AIS spine and its bone formation effects. **a** GPR126 contains 26 exons, and alternative splicing of exon6 and exon25 produces four protein-coding transcript variants (TVs). **b** and **c** The expression pattern of GPR126-transcripts in the convex/concave side of the AIS spine. The expression levels of exon6-included transcripts (GPR126-exon6^{in}, TV-a1, b1) in the convex side were significantly higher than concave side, and there was no significant difference in the expression levels of exon6-excluded transcripts (GPR126-exon6^{ex}, TV-a2, b2) in two sides of AIS spine. $n=51$. **d** and **e** Osteogenic differentiation and RT-qPCR detection for untreated hMSCs. The expression levels of GPR126-exon6^{in} decreased during osteogenic differentiation, but this result was not observed in GPR126-exon6^{ex}. **f** and **g** Four GPR126-transcript variants were overexpressed in hMSCs (TV-a1, b1, a2, b2). The expression levels of GPR126-exon6^{in} in TV-a1 and b1 were significantly higher than TV-a2 and b2. Delayed osteogenic differentiation was observed in the TV-a1 and b1. Data were presented as the mean ± SD. $^{**}P<0.01$, $^{***}P<0.001$

and cancellous at the concave side was higher than the convex side [4].

Some studies have investigated the causes of AIS skeletal abnormalities. Primary osteoblasts derived from AIS showed abnormal osteogenic differentiation ability and differentiated gene expression [27–29]. Some bone growth and development-related factors like MAPK7, DPP-4, melatonin, Runx2, lncAIS (a novel AIS-related long noncoding RNA), miRNA-145-5p and other miRNAs were found to be associated with AIS [30–36]. Cells derived from idiopathic scoliosis patients differentially express osteogenic factors response to mechanical stimulation with significant primary cilia elongation [37]. Osteoblasts are related to the mineralization, the mechanical strengthening of bone and inhibition of the osteoclastic bone resorption [38–40]. The correct balance of osteoblastic/osteoclastic signals is crucial in spinal maturation. Some researchers suggest that the low bone mass in AIS is a systemic phenomenon that may be

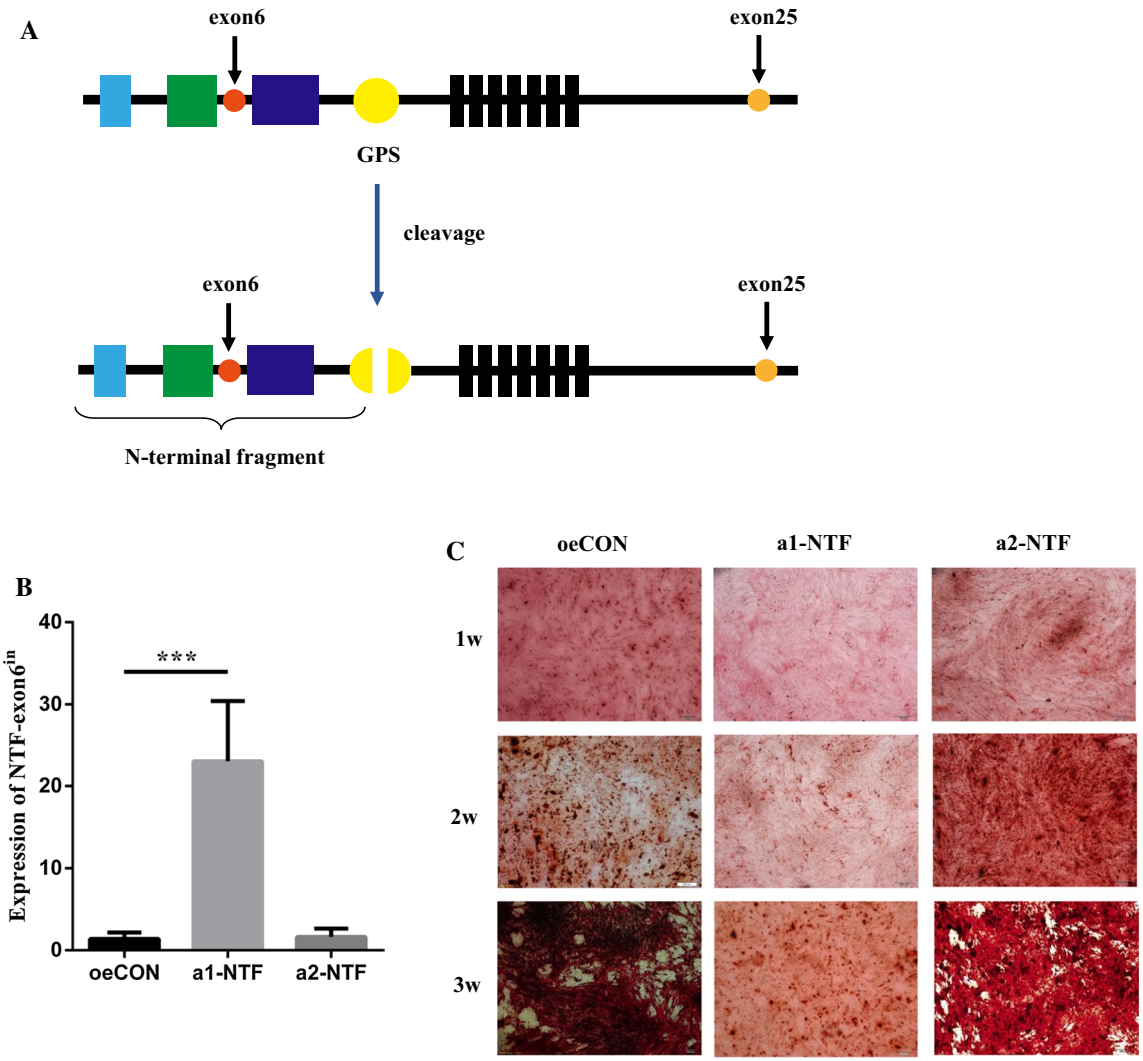

Fig. 3 Skeletal development-related functions of GPR126-NTFs. **a** GPR126 is cleaved at the GPS motif into a N-terminal fragment (NTF) that locates to the plasma membrane. **b** and **c** Two GPR126-NTFs were overexpressed in hMSCs (a1-NTF, a2-NTF). The expression level of exon6-included NTF (NTF-exon6^{in}) in a1-NTF was significantly higher than a2-NTF. Delayed osteogenic differentiation was observed in the a1-NTF. Data were presented as the mean ± SD. ***$P < 0.001$

attributable to impaired osteoblast and osteocyte activities [35].

However, the etiology and pathogenesis of AIS are still uncertain right now [41], and some studies have reported that GPR126 is associated with AIS [14–17]. However, there is no research to explore the specific functions of the GPR126 in the development of spinal deformity. Compared with the lumbar disk herniation (LDH) controls, GPR126 expression in vertebral body was significantly higher in patients with AIS [16]. Recently study suggests that GPR126 increased the expression of bone sialoprotein, osteopontin and Runx2 through the GPR126-induced increase of BMP2, inhibitor of DNA binding 2 (ID2) and ID4 expression in human periodontal ligament (HPDL) cells [42]. In our study, GPR 126 was found to have a significantly higher expression on the concave side than the concave side of AIS patients in our department. We suspected that asymmetric expression of GPR126 in the convex/concave side of the spine may be associated with the abnormal bone formation of patients with AIS.

GPR126 contains 26 exons, and alternative splicing of exon6 and exon25 produces four protein-coding transcripts. Alternative splicing is associated with multiple diseases [43–45]. Some studies have shown that alternative splicing is associated with intracellular localization and function of protein. The Liptin gene can be translated into an isoform located in the nucleus and a cytoplasmic isoform, the former being a transcription factor and the latter having phosphatase activity [46, 47]. Typically, the erythropoietin receptor is a membrane protein, but one of

its splicing isoforms is a soluble protein [48]. The ability of proteins to bind to other proteins will change due to alternative splicing. An insulin splicing isoform (exon11 skips) showed abnormally high affinity for IGF-II [49]. In our study, the expression levels of exon6-included transcripts (GPR126-exon6^{in}, TV-a1, b1) in convex side were significantly higher than concave side, and there was no significant difference in the expression levels of exon6-excluded transcripts (GPR126-exon6^{ex}, TV-a2, b2) in two sides of AIS spine. The expression levels of GPR126-exon6^{in} decreased during osteogenic differentiation of untreated hMSCs, but this result was not observed in GPR126-exon6^{ex}. Overexpression and differentiation experiments showed delayed osteogenic differentiation in the TV-a1 and b1 overexpressing cell lines.

GPR126 is cleaved at the GPS motif into a N-terminal fragment (NTF) that locates to the plasma membrane [23]. NTF contains a CUB (Complement, Uegf, Bmp1) domain, a pentraxin domain, a hormone-binding domain and 27 putative N-glycosylation sites [23, 50, 51] and works by interacting with neighboring cells or extracellular matrix [24]. Researchers found that NTFs derived from GPR126 were associated with cardiac development [52], but no studies have shown a correlation between NTFs and skeletal development. We first provided evidence that NTFs were involved in bone formation in hMSCs, and delayed osteogenic differentiation was observed in the a1-NTF overexpression cell line.

In summary, we provided evidence that GPR126 showed a marked convex/concave asymmetric expression in the spine of AIS. Exon6-included transcripts of GPR126 were found to be factors that delay ossification and were expressed at higher levels in the convex side of the AIS spine. In addition, the NTFs derived from GPR126 play a role in skeletal development, and exon6-included NTF may be a major factor in GPR126 bone formation-related functions.

This is a limited research because we did not determine the differences of GPR126 expression in vertebral body samples from patients with AIS and those without spinal deformity. It is difficult to obtain vertebral body samples from adolescents whose age and gender match AIS, because few adolescents with non-spinal deformities require spinal surgery in our department. Only one study has investigated the difference in GPR126 expression levels in vertebral bone between AIS patients and controls. The researchers found that the expression level of GPR126 in the vertebral bone of AIS patients was significantly higher, but the sample size was small (eight patients and five controls) [16]. We plan to enroll patients without spinal deformity in future studies to further determine the effects of GPR126 transcript variants on spinal bone formation.

Compliance with ethical standards

Conflict of interest The authors declare that they have no conflict of interest.

References

1. Xiong B, Sevastik B, Sevastik J, Hedlund R, Suliman I, Kristjansson S (1995) Horizontal plane morphometry of normal and scoliotic vertebrae. A methodological study. Eur Spine J 4(1):6–10
2. Xiong B, Sevastik B, Willers U, Sevastik J, Hedlund R (1995) Structural vertebral changes in the horizontal plane in idiopathic scoliosis and the long-term corrective effect of spine instrumentation. Eur Spine J 4(1):11–14
3. Liljenqvist UR, Allkemper T, Hackenberg L, Link TM, Steinbeck J, Halm HF (2002) Analysis of vertebral morphology in idiopathic scoliosis with use of magnetic resonance imaging and multiplanar reconstruction. J Bone Joint Surg Am 84-A(3):359–368
4. Adam CJ, Askin GN (2009) Lateral bone density variations in the scoliotic spine. Bone 45(4):799–807. https://doi.org/10.1016/j.bone.2009.06.023
5. Millner PA, Dickson RA (1996) Idiopathic scoliosis: biomechanics and biology. Eur Spine J 5(6):362–373
6. Yim AP, Yeung HY, Hung VW, Lee KM, Lam TP, Ng BK, Qiu Y, Cheng JC (2012) Abnormal skeletal growth patterns in adolescent idiopathic scoliosis—a longitudinal study until skeletal maturity. Spine (Phila Pa 1976) 37(18):E1148–E1154. https://doi.org/10.1097/brs.0b013e31825c036d
7. Lee WT, Cheung CS, Tse YK, Guo X, Qin L, Ho SC, Lau J, Cheng JC (2005) Generalized low bone mass of girls with adolescent idiopathic scoliosis is related to inadequate calcium intake and weight bearing physical activity in peripubertal period. Osteoporos Int J Establ Result Cooperation Betw Eur Found Osteoporos Natl Osteoporos Found USA 16(9):1024–1035. https://doi.org/10.1007/s00198-004-1792-1
8. Chiru M (2011) Adolescent idiopathic scoliosis and osteopenia). Maedica 6(1):17–22
9. Sadat-Ali M, Al-Othman A, Bubshait D, Al-Dakheel D (2008) Does scoliosis causes low bone mass? A comparative study between siblings. Eur Spine J 17(7):944–947. https://doi.org/10.1007/s00586-008-0671-4
10. Hung VW, Qin L, Cheung CS, Lam TP, Ng BK, Tse YK, Guo X, Lee KM, Cheng JC (2005) Osteopenia: a new prognostic factor of curve progression in adolescent idiopathic scoliosis. J Bone Joint Surg Am 87(12):2709–2716. https://doi.org/10.2106/JBJS.D.02782
11. Yu WS, Chan KY, Yu FW, Ng BK, Lee KM, Qin L, Lam TP, Cheng JC (2014) Bone structural and mechanical indices in Adolescent Idiopathic Scoliosis evaluated by high-resolution peripheral quantitative computed tomography (HR-pQCT). Bone 61:109–115. https://doi.org/10.1016/j.bone.2013.12.033
12. Wang Z, Chen H, Yu YE, Zhang J, Cheuk KY, Ng BK, Qiu Y, Guo XE, Cheng JC, Lee WY (2017) Unique local bone tissue characteristics in iliac crest bone biopsy from adolescent idiopathic scoliosis with severe spinal deformity. Sci Rep 7:40265. https://doi.org/10.1038/srep40265
13. Tam EM, Yu FW, Hung VW, Liu Z, Liu KL, Ng BK, Lee SK, Qiu Y, Cheng JC, Lam TP (2014) Are volumetric bone mineral density and bone micro-architecture associated with leptin and soluble leptin receptor levels in adolescent idiopathic scoliosis?—A case-control study. PLoS ONE 9(2):e87939. https://doi.org/10.1371/journal.pone.0087939

14. Kou I, Takahashi Y, Johnson TA, Takahashi A, Guo L, Dai J, Qiu X, Sharma S, Takimoto A, Ogura Y, Jiang H, Yan H, Kono K, Kawakami N, Uno K, Ito M, Minami S, Yanagida H, Taneichi H, Hosono N, Tsuji T, Suzuki T, Sudo H, Kotani T, Yonezawa I, Londono D, Gordon D, Herring JA, Watanabe K, Chiba K, Kamatani N, Jiang Q, Hiraki Y, Kubo M, Toyama Y, Tsunoda T, Wise CA, Qiu Y, Shukunami C, Matsumoto M, Ikegawa S (2013) Genetic variants in GPR126 are associated with adolescent idiopathic scoliosis. Nat Genet 45(6):676–679
15. Xu JF, Yang GH, Pan XH, Zhang SJ, Zhao C, Qiu BS, Gu HF, Hong JF, Cao L, Chen Y, Xia B, Bi Q, Wang YP (2015) Association of GPR126 gene polymorphism with adolescent idiopathic scoliosis in Chinese populations. Genomics 105(2):101–107
16. Qin X, Xu L, Xia C, Zhu W, Sun W, Liu Z, Qiu Y, Zhu Z (2017) Genetic variant of GPR126 gene is functionally associated with adolescent idiopathic scoliosis in Chinese population. Spine (Phila Pa 1976) 42(19):E1098–E1103. https://doi.org/10.1097/brs.0000000000002123
17. Liu G, Liu S, Lin M, Li X, Chen W, Zuo Y, Liu J, Niu Y, Zhao S, Long B, Wu Z, Wu N, Qiu G (2018) Genetic polymorphisms of GPR126 are functionally associated with PUMC classifications of adolescent idiopathic scoliosis in a Northern Han population. J Cell Mol Med 22:1964–1971
18. Lettre G, Jackson AU, Gieger C, Schumacher FR, Berndt SI, Sanna S, Eyheramendy S, Voight BF, Butler JL, Guiducci C, Illig T, Hackett R, Heid IM, Jacobs KB, Lyssenko V, Uda M, Boehnke M, Chanock SJ, Groop LC, Hu FB, Isomaa B, Kraft P, Peltonen L, Salomaa V, Schlessinger D, Hunter DJ, Hayes RB, Abecasis GR, Wichmann HE, Mohlke KL, Hirschhorn JN (2008) Identification of ten loci associated with height highlights new biological pathways in human growth. Nat Genet 40(5):584–591
19. Soranzo N, Rivadeneira F, Chinappen-Horsley U, Malkina I, Richards JB, Hammond N, Stolk L, Nica A, Inouye M, Hofman A, Stephens J, Wheeler E, Arp P, Gwilliam R, Jhamai PM, Potter S, Chaney A, Ghori MJ, Ravindrarajah R, Ermakov S, Estrada K, Pols HA, Williams FM, McArdle WL, van Meurs JB, Loos RJ, Dermitzakis ET, Ahmadi KR, Hart DJ, Ouwehand WH, Wareham NJ, Barroso I, Sandhu MS, Strachan DP, Livshits G, Spector TD, Uitterlinden AG, Deloukas P (2009) Meta-analysis of genome-wide scans for human adult stature identifies novel Loci and associations with measures of skeletal frame size. PLoS Genet 5(4):e1000445
20. Sovio U, Bennett AJ, Millwood IY, Molitor J, O'Reilly PF, Timpson NJ, Kaakinen M, Laitinen J, Haukka J, Pillas D, Tzoulaki I, Molitor J, Hoggart C, Coin LJ, Whittaker J, Pouta A, Hartikainen AL, Freimer NB, Widen E, Peltonen L, Elliott P, McCarthy MI, Jarvelin MR (2009) Genetic determinants of height growth assessed longitudinally from infancy to adulthood in the northern Finland birth cohort 1966. PLoS Genet 5(3):e1000409
21. Zhao J, Li M, Bradfield JP, Zhang H, Mentch FD, Wang K, Sleiman PM, Kim CE, Glessner JT, Hou C, Keating BJ, Thomas KA, Garris ML, Deliard S, Frackelton EC, Otieno FG, Chiavacci RM, Berkowitz RI, Hakonarson H, Grant SF (2010) The role of height-associated loci identified in genome wide association studies in the determination of pediatric stature. BMC Med Genet 11:96
22. Monk KR, Oshima K, Jors S, Heller S, Talbot WS (2011) Gpr126 is essential for peripheral nerve development and myelination in mammals. Development 138(13):2673–2680
23. Moriguchi T, Haraguchi K, Ueda N, Okada M, Furuya T, Akiyama T (2004) DREG, a developmentally regulated G protein-coupled receptor containing two conserved proteolytic cleavage sites. Genes Cells 9(6):549–560. https://doi.org/10.1111/j.1356-9597.2004.00743.x
24. Langenhan T, Aust G, Hamann J (2013) Sticky signaling–adhesion class G protein-coupled receptors take the stage. Sci Signal 6(276):re3. https://doi.org/10.1126/scisignal.2003825
25. Yip BH, Yu FW, Wang Z, Hung VW, Lam TP, Ng BK, Zhu F, Cheng JC (2016) Prognostic value of bone mineral density on curve progression: a longitudinal cohort study of 513 girls with adolescent idiopathic scoliosis. Sci Rep 6:39220. https://doi.org/10.1038/srep39220
26. Tanabe H, Aota Y, Yamaguchi Y, Kaneko K, Imai S, Takahashi M, Taguri M, Saito T (2018) Minodronate treatment improves low bone mass and reduces progressive thoracic scoliosis in a mouse model of adolescent idiopathic scoliosis. PLoS ONE 13(8):e0202165. https://doi.org/10.1371/journal.pone.0202165
27. Suh KT, Lee SS, Hwang SH, Kim SJ, Lee JS (2007) Elevated soluble receptor activator of nuclear factor-κB ligand and reduced bone mineral density in patients with adolescent idiopathic scoliosis. Eur Spine J 16(10):1563–1569. https://doi.org/10.1007/s00586-007-0390-2
28. Man GC, Wong JH, Wang WW, Sun GQ, Yeung BH, Ng TB, Lee SK, Ng BK, Qiu Y, Cheng JC (2011) Abnormal melatonin receptor 1B expression in osteoblasts from girls with adolescent idiopathic scoliosis. J Pineal Res 50(4):395–402. https://doi.org/10.1111/j.1600-079X.2011.00857.x
29. Fendri K, Patten SA, Kaufman GN, Zaouter C, Parent S, Grimard G, Edery P, Moldovan F (2013) Microarray expression profiling identifies genes with altered expression in adolescent idiopathic scoliosis. Eur Spine J 22(6):1300–1311. https://doi.org/10.1007/s00586-013-2728-2
30. Zhuang Q, Li J, Wu Z, Zhang J, Sun W, Li T, Yan Y, Jiang Y, Zhao RC, Qiu G (2011) Differential proteome analysis of bone marrow mesenchymal stem cells from adolescent idiopathic scoliosis patients. PLoS ONE 6(4):e18834. https://doi.org/10.1371/journal.pone.0018834
31. Zhou T, Chen C, Xu C, Zhou H, Gao B, Su D, Liao Z, Li Y, Yang S, Su P (2018) Mutant MAPK7-induced idiopathic scoliosis is linked to impaired osteogenesis. Cell Physiol Biochem Int J Exp Cell Physiol Biochem Pharmacol 48(3):880–890. https://doi.org/10.1159/000491956
32. Normand E, Franco A, Moreau A, Marcil V (2017) Dipeptidyl peptidase-4 and adolescent idiopathic scoliosis: expression in osteoblasts. Sci Rep 7(1):3173. https://doi.org/10.1038/s41598-017-03310-x
33. Man GC, Wang WW, Yeung BH, Lee SK, Ng BK, Hung WY, Wong JH, Ng TB, Qiu Y, Cheng JC (2010) Abnormal proliferation and differentiation of osteoblasts from girls with adolescent idiopathic scoliosis to melatonin. J Pineal Res 49(1):69–77. https://doi.org/10.1111/j.1600-079X.2010.00768.x
34. Zhuang Q, Ye B, Hui S, Du Y, Zhao RC, Li J, Wu Z, Li N, Zhang Y, Li H, Wang S, Yang Y, Li S, Zhao H, Fan Z, Qiu G, Zhang J (2018) Long noncoding RNA lncAIS downregulation in mesenchymal stem cells is implicated in the pathogenesis of adolescent idiopathic scoliosis. Cell Death Differ. https://doi.org/10.1038/s41418-018-0240-2
35. Zhang J, Chen H, Leung RKK, Choy KW, Lam TP, Ng BKW, Qiu Y, Feng JQ, Cheng JCY, Lee WYW (2018) Aberrant miR-145-5p/β-catenin signal impairs osteocyte function in adolescent idiopathic scoliosis. FASEB J 45:45. https://doi.org/10.1096/fj.201800281
36. Garcia-Gimenez JL, Rubio-Belmar PA, Peiro-Chova L, Hervas D, Gonzalez-Rodriguez D, Ibanez-Cabellos JS, Bas-Hermida P, Mena-Molla S, Garcia-Lopez EM, Pallardo FV, Bas T (2018) Circulating miRNAs as diagnostic biomarkers for adolescent idiopathic scoliosis. Sci Rep 8(1):2646. https://doi.org/10.1038/s41598-018-21146-x
37. Oliazadeh N, Gorman KF, Eveleigh R, Bourque G, Moreau A (2017) Identification of elongated primary cilia with impaired mechanotransduction in idiopathic scoliosis patients. Sci Rep 7:44260. https://doi.org/10.1038/srep44260

38. Bonewald LF, Johnson ML (2008) Osteocytes, mechanosensing and Wnt signaling. Bone 42(4):606–615. https://doi.org/10.1016/j.bone.2007.12.224
39. Ozcivici E, Luu YK, Adler B, Qin YX, Rubin J, Judex S, Rubin CT (2010) Mechanical signals as anabolic agents in bone. Nat Rev Rheumatol 6(1):50–59. https://doi.org/10.1038/nrrheum.2009.239
40. Harada S, Rodan GA (2003) Control of osteoblast function and regulation of bone mass. Nature 423(6937):349–355. https://doi.org/10.1038/nature01660
41. Pollak L, Shlamkovic N, Minewicz A, Mirovsky Y (2013) Otolith dysfunction as a possible cause for the development of idiopathic scoliosis. J Pediatr Orthop 33(3):293–297
42. Kitagaki J, Miyauchi S, Asano Y, Imai A, Kawai S, Michikami I, Yamashita M, Yamada S, Kitamura M, Murakami S (2016) A putative association of a single nucleotide polymorphism in GPR126 with aggressive periodontitis in a Japanese population. PLoS ONE 11(8):e0160765. https://doi.org/10.1371/journal.pone.0160765
43. Lorson CL, Hahnen E, Androphy EJ, Wirth B (1999) A single nucleotide in the SMN gene regulates splicing and is responsible for spinal muscular atrophy. Proc Natl Acad Sci USA 96(11):6307–6311
44. Albert H, Santos S, Battaglia E, Brito M, Monteiro C, Bagrel D (2011) Differential expression of CDC25 phosphatases splice variants in human breast cancer cells. Clin Chem Lab Med 49(10):1707–1714. https://doi.org/10.1515/CCLM.2011.635
45. Wang Y, Chan DW, Liu VW, Chiu P, Ngan HY (2010) Differential functions of growth factor receptor-bound protein 7 (GRB7) and its variant GRB7v in ovarian carcinogenesis. Clin Cancer Res 16(9):2529–2539. https://doi.org/10.1158/1078-0432.CCR-10-0018
46. Han GS, Carman GM (2010) Characterization of the human LPIN1-encoded phosphatidate phosphatase isoforms. J Biol Chem 285(19):14628–14638. https://doi.org/10.1074/jbc.M110.117747
47. Zhang P, Takeuchi K, Csaki LS, Reue K (2012) Lipin-1 phosphatidic phosphatase activity modulates phosphatidate levels to promote peroxisome proliferator-activated receptor gamma (PPARgamma) gene expression during adipogenesis. J Biol Chem 287(5):3485–3494. https://doi.org/10.1074/jbc.M111.296681
48. Khankin EV, Mutter WP, Tamez H, Yuan HT, Karumanchi SA, Thadhani R (2010) Soluble erythropoietin receptor contributes to erythropoietin resistance in end-stage renal disease. PLoS ONE 5(2):e9246. https://doi.org/10.1371/journal.pone.0009246
49. Belfiore A, Frasca F, Pandini G, Sciacca L, Vigneri R (2009) Insulin receptor isoforms and insulin receptor/insulin-like growth factor receptor hybrids in physiology and disease. Endocr Rev 30(6):586–623. https://doi.org/10.1210/er.2008-0047
50. Fredriksson R, Gloriam DE, Hoglund PJ, Lagerstrom MC, Schioth HB (2003) There exist at least 30 human G-protein-coupled receptors with long Ser/Thr-rich N-termini. Biochem Biophys Res Commun 301(3):725–734
51. Stehlik C, Kroismayr R, Dorfleutner A, Binder BR, Lipp J (2004) VIGR—a novel inducible adhesion family G-protein coupled receptor in endothelial cells. FEBS Lett 569(1–3):149–155. https://doi.org/10.1016/j.febslet.2004.05.038
52. Patra C, van Amerongen MJ, Ghosh S, Ricciardi F, Sajjad A, Novoyatleva T, Mogha A, Monk KR, Muhlfeld C, Engel FB (2013) Organ-specific function of adhesion G protein-coupled receptor GPR126 is domain-dependent. Proc Natl Acad Sci USA 110(42):16898–16903. https://doi.org/10.1073/pnas.1304837110

Publisher's Note Springer Nature remains neutral with regard to jurisdictional claims in published maps and institutional affiliations.

Affiliations

Enjie Xu[1] · Tao Lin[1] · Heng Jiang[1] · Zhe Ji[1] · Wei Shao[1] · Yichen Meng[1] · Rui Gao[1] · Xuhui Zhou[1]

✉ Rui Gao
rgaospine@163.com

✉ Xuhui Zhou
xhzhouspine@163.com

[1] Department of Orthopedics, Changzheng Hospital, Second Affiliated Hospital of Second Military Medical University, No. 415 Fengyang Road, Shanghai, People's Republic of China